

Representation of seasonal land-use dynamics in SWAT+ for improved assessment of blue and green water consumption

Anna Msigwa^{1,2}, Celray James Chawanda², Hans C. Komakech¹, Albert Nkwasa², and Ann van Griensven^{2,3}

5 ¹The Nelson Mandela African Institution of Science and Technology, Arusha 447, Tanzania

² Department of Hydrology and Hydraulic Engineering, Vrije Universiteit, Pleinlaan 2 -1050, 1050 Brussel, Belgium

³ IHE-Delft Institute for Water Education; Westvest 7, 2611 AX Delft, The Netherlands

Correspondence to: Anna Msigwa (anna.msigwa@nm-aist.ac.tz)

Abstract. In most (sub)-tropical African cultivated regions, more than one cropping season exists following the (one or two) rainy seasons. During the dry season, an additional cropping season is possible when irrigation is applied, which could result in 3 cropping seasons. However, most studies for mapping the blue and green ET with agro-hydrological models such as SWAT do not represent these cropping seasons. Blue ET is a portion of crop evapotranspiration after application of irrigation while green ET is the evapotranspiration as a result of rainfall. In this paper, we derived dynamic and static trajectories from seasonal land-use maps to represent the land-use dynamics following the major growing seasons, for the purpose of improving simulated blue and green water consumption from simulated evapotranspiration (ET) in SWAT+. A comparison between the default SWAT+ (with static land use representation) set up, and a dynamic SWAT+ model (with seasonal land use representation) is done by spatial mapping of ET results. Additionally, the SWAT+ blue and green ET were compared with the results from the four remote sensing data-based methods namely: SN (Senay), EK (van Eekelen), Budyko method and Soil Water Balance method (SWB). The results show that ET with seasonal representation is closer to remote sensing estimates, giving higher performance than ET with static land use representation.: The Root Mean Squared Error decreased from 181 to 69 mm/year; the percent bias decreased from 20 % to 13% and Nash Sutcliffe Efficiency increased from -0.46 to 0.4. Further the results of blue and green ET from the dynamic SWAT+ model were compared to the four remote sensing methods. The results shows that the SWAT+ blue and green ET are similar to the van Eekelen method that performed better than the other three remote sensing methods. It is concluded that representation of seasonal land-use dynamics produces better ET results which provide better estimations of blue and green agricultural water consumption.

1. Introduction

Freshwater availability is a limiting resource in many regions throughout the world and the problem is projected to increase in the near future due to land use change, population growth, and climate change. The availability of freshwater is mostly determined by precipitation on land. When rain falls on

30 land, it travels via either green or blue waterways (Velpuri and Senay, 2017; Hoekstra, 2019). The green

water resource is the water that is held in the unsaturated soil layer, whereas the blue water resource is the water that is stored in rivers, streams, surface-water bodies, and groundwater (Falkenmark and Rockström, 2006). One of the solutions to lessen the threat of freshwater scarcity is to minimize consumptive water use in agriculture. However, for water resource management, it is critical to understand water use in agricultural production by source (rainwater or irrigation water from surface and groundwater) (Velpuri and Senay, 2017). For efficient water resource management, knowing how much direct rainwater (green water) and abstracted water (blue water) is being utilized is crucial. Yet such information is not readily available, especially in developing countries.

Hydrological models such as the Soil Water Assessment Tool (SWAT) can be used to provide information on blue and green water at basin and continental scales (Xie et al., 2020; Jeyrani et al., 2021; Liang et al., 2020; Serur, 2020). For instance, Schuol et al. (2008) used the SWAT model to simulate blue and green water availability for the African continent. Xie et al. (2020), evaluated the evolution of the blue and green water resources, water footprints, and water scarcities in time and space in the Yellow River basin in China from 2010–2018. The study accounts for the effects of irrigation on blue and green water resources. Liang et al. (2020) used the SWAT model combined with future land use and climate scenarios, which was successfully applied to quantify the spatiotemporal distribution of blue and green water change for the Xiangjiang River Basin in China between 2015 and 2050.

However, a few of these studies have implemented annual land-use dynamics. Since land-use refers to manmade socio-economic activities and management practices on the land, these anthropogenic activities may change depending on a season, specifically on cultivated land (Anderson et al., 1976). These changes per season are called seasonal land-use dynamics (Msigwa et al., 2019). Hence, mapping the blue and green water with agro-hydrological models such as SWAT need a better representation of the seasonality/cropping seasons. To best of our knowledge there are no studies that implemented seasonal land-use dynamics in estimation of blue and green water resources. For example, Jeyran et al. (2021), assessed basin blue and green available water components under different management and climatic scenario using SWAT. The annual land-use change implementation showed that the 30% increase in agricultural land use from 1987 to 2015 has caused significant changes in water shortages of Tashk-

Bakhtegan basin in Iran. However, other studies do not implement even the annual land-use dynamic in order to decrease the computational time of the very large-scale models. In most cases, the dominant soil 60 and land cover are used. For instance, Serur (2020) used a 10-year land use map to model blue and green water availability for the Weyb River basin in Ethiopia.

The major limitation of applying these approaches in tropical African cultivated areas is that typically they have more than one growing cycle, most of the time ranging between 2 to 3 depending on the sequence of rainy and dry seasons and availability of irrigation water (Msigwa et al., 2019). The right 65 representation and timing of these cropping seasons is therefore important in order to quantify the crop water consumption.

A Few studies that have implemented seasonal land-use dynamic for other purposes such as nitrogen leaching and plant growth (Glavan et al., 2015), estimating water withdrawals (Msigwa et al., 2019) and Leaf Area Index (LAI) simulation (Nkwasa et al., 2020), have found an impact of representing seasonal 70 land-use dynamics in models. For instance, Nkwasa et al. (2020) found that the implementation of seasonal land-use dynamics in SWAT and SWAT+ models led to an improved vegetation simulation. The LAI dynamics of the seasonal land-use dynamic implementation showed more realistic temporal advancement patterns that corresponded to the seasonal rainfall within the basin. Moreover, Msigwa et al. (2019) found that water withdrawals for irrigated mixed crops increased by 482 Mm³/year when 75 seasonal land-use maps are used. On the other hand, the seasonal land use-dynamics have been studied and evaluated using four methods that use multi-scalar datasets to assess cropping intensity of smallholder farms. In this study, the cropping intensity is the number of crops planted annually (Jain et al., 2013). However, in this case, the impact of seasonal land use on water resources has not been studied.

The SWAT model incorporates crop rotation and its management at the level of the Hydrological 80 Response Unit (HRU) within a sub-basin (Neitsch et al., 2002). It is represented as a sequence of planting and harvesting operations within the same HRU supplemented with management operations (Gao et al., 2017). The representation of agricultural management is done through a separate management file by specifying the planting, harvesting, tillage, irrigation, fertilizer and pesticide application by heat units or

month and date (Arnold et al., 2018). Although, the SWAT (+) model is capable of representing multiple 85 cropping seasons, however this is mainly implemented outside Africa catchments. Agro-hydrological model applications in Africa basins do typically not represent different cropping seasons. Rather implement the default SWAT simulation of a single growing cycle every year (Ndomba et al., 2008; Koch et al., 2012; Gashaw et al., 2018). Lack of consideration of the seasonal land-use dynamics in hydrologic 90 modelling studies, especially in African cultivated basins, may be attributed to past constraints of model capabilities, as well as lack of availability of crop-specific and agricultural management practices data (van Griensven et al., 2012).

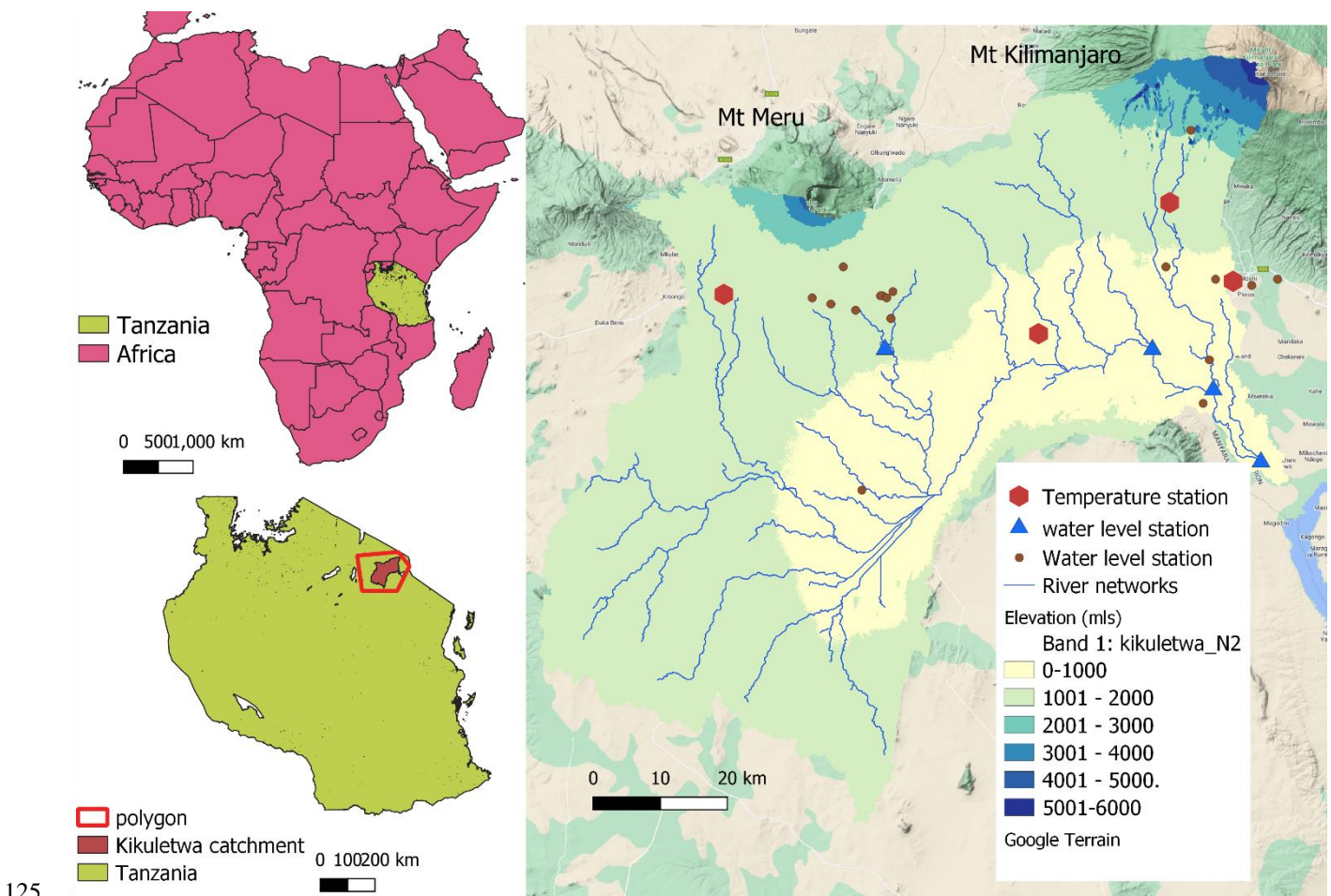
Hence, the crop-specific and data management practices could be obtained from the seasonal land use maps using trajectory analysis. Trajectories represent changes of land-use over time by comparing 95 changes between two or several land-use maps at a grid scale. Trajectory analysis has been applied widely to assess the changes and impact of Land Use and Land Cover (LULC) (Feng et al., 2014; Wang et al., 2012), and as a pre-processing tool for LULC (Zomlot et al., 2017). In these studies, change analysis is done pixel by pixel for each year in order to identify land use change (Mertens and Lambin, 2000; Swetnam, 2007; Zhou et al., 2008; Wang et al., 2012; Zomlot et al., 2017). However, none of these studies 100 have analysed pixel by pixel within a year with the aim of identifying the different (cropping) seasons, further referred to as land use dynamics.

A recent study by Nkwasa et al. (2020) in the Usa catchment with in Kikuletwa basin in northern Tanzania has shown how to represent seasonal land-use dynamics using trajectories in the SWAT model using the management file and the SWAT+ model using decision tables for accurate hydrological simulation. This 105 study builds on Nkwasa et al. (2020) approach to evaluate the effects of seasonal land-use dynamics on blue and green ET, with two main objectives; (i) investigate the effect of implementing seasonal land-use dynamics on the water balance component in Kikuletwa basin (6650 km^2) with focus on the ET using SWAT+ and (ii) to estimate blue and green water consumption from simulated ET.

2. Methods

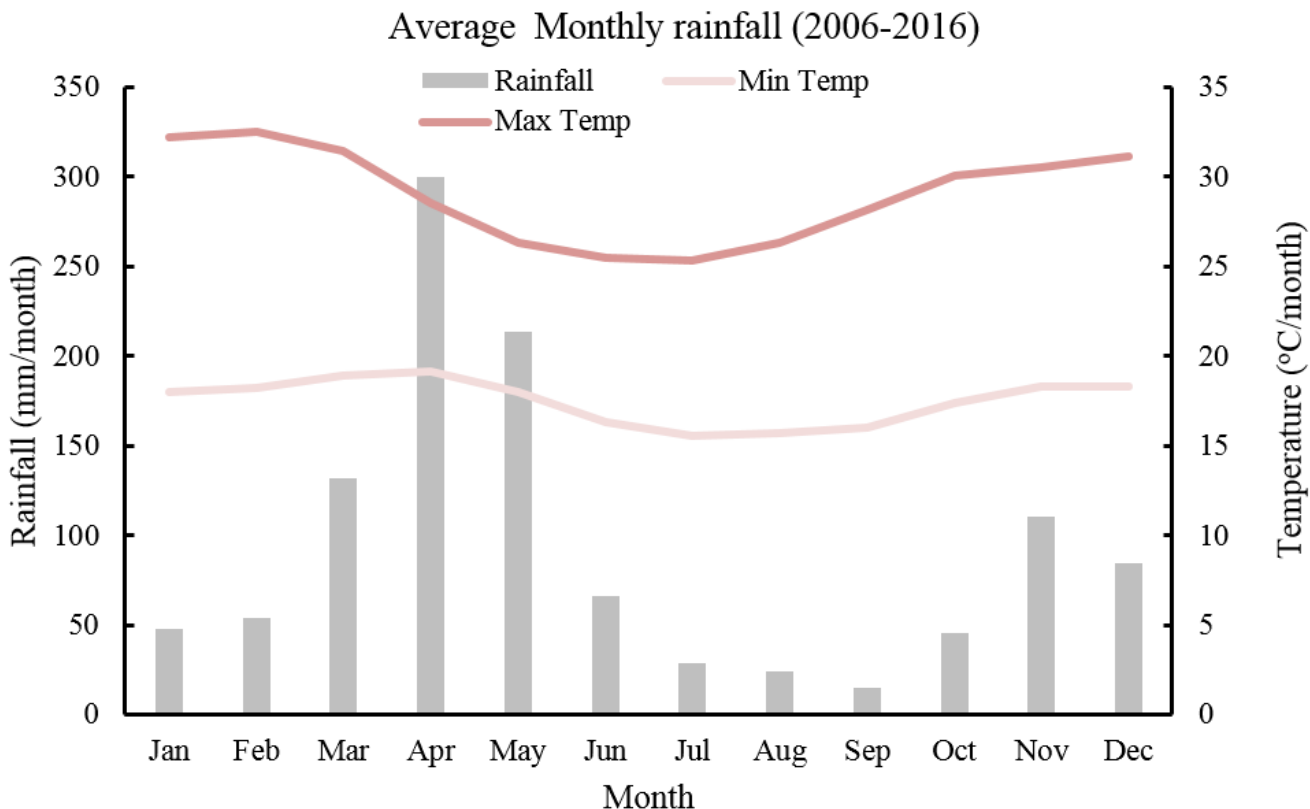
110 2.1. Study Area

The Kikuletwa basin is a sub-basin of the Pangani basin that covers approximately 6,650 km² (Figure 1). Rainfall within the basin is bimodal, meaning that the area receives long rains (Masika) from March to June and short rains (Vuli) from November to December, as shown in Figure 2. Annual rainfall ranges between 300-800 mm in the lower part of the basin to 1200-2000 mm in the highlands of Mount Meru 115 and Kilimanjaro. The maximum temperature ranges from 25 to 33⁰C and minimum temperature ranges from 15 to 20⁰C. The basin comprises of diverse LULC classes such as agricultural land, dense forest on Mount Kilimanjaro (5880m) and Meru (4562m), grazed land, mixed urban and shrubland/thickets. Shrubland and thickets in the study area are found mainly in the lowlands where rain-fed agriculture is dominant. Urban areas concentrate around Arusha, although there are also emerging small towns. 120 Moreover, grazed land is mainly found in the Maasai land of Monduli and Simanjiro districts. Irrigated agriculture in Kikuletwa is mainly practiced in the highlands and lowlands along the river of Moshi, Moshi urban, Hai, Arumeru, Arusha, and Siha districts. The main crops in the highlands are banana, coffee, and maize, while the lowlands are dominated by mixed vegetable crops such as tomatoes, onions, and beans.



125

Figure 1. The location of the Kikuletwa catchment in Africa (inset map). The catchment map shows the river networks and the location of ground water level, rainfall and temperature station in and around the catchment. (by Authors).



130 **Figure 2.** Monthly average rainfall (mm) and temperature of Kikuletwa basin ground rainfall stations

2.2 Input dataset for SWAT+

The required rainfall, river discharge, climate data, topography, soil map and land-use map were collected from different sources. The 90-m Shuttle Radar Topographic Mission (SRTM) Digital Elevation Model (DEM) was obtained from the United States Geological Survey (USGS) website 135 (<https://earthexplorer.usgs.gov/>); the soil map was extracted from the African Soil Information Service (AFSIS; Hengl et al., 2015). Daily rainfall records for 10 stations were obtained from the Tanzania Meteorological Agency (TMA) and Pangani Basin Water Office (PBWO). The daily climate records of temperature (maximum and minimum) for three stations were obtained from PBWO and TMA. The different data sets had variable record length and quality. However, for the selected 10 rainfall and 4

140 temperature stations, only good quality data records for the overlapping period (2006 to 2013) were selected.

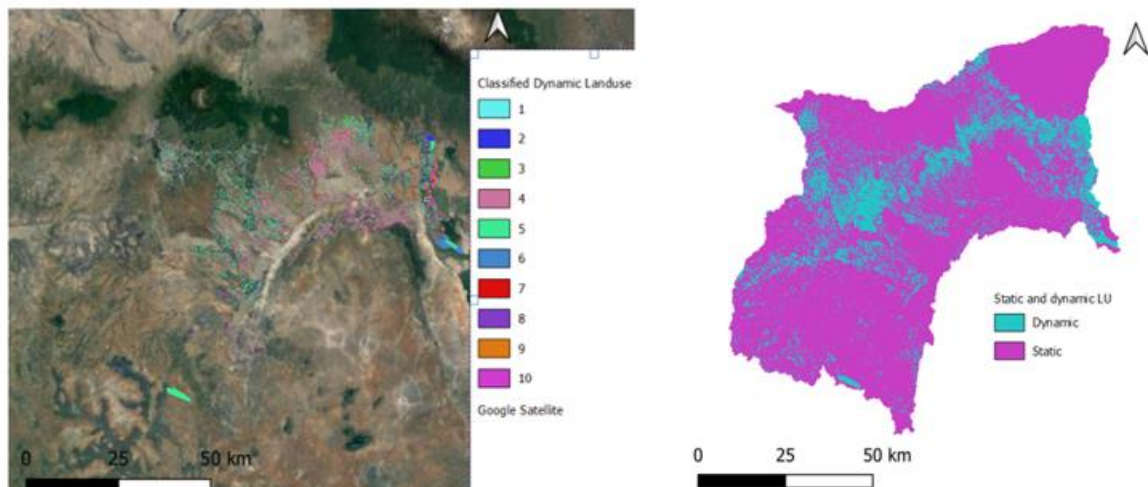
Our study used an improved LULC maps with local observation unlike other studies in the same catchment such as (Notter et al., 2012; Ndomba et al., 2008). For instance, Notter et al. 2012 used only a few herbaceous crops in model parametrization without a cropping calendar. The LULC maps were 145 created using Landsat 8 (30m resolution) image of three months (March, August and October) representing three seasons in the basin. The March map represents the LULC during the long-wet season (*Masika*), the August map represents the dry season, and the October map represents the short rainy seasons (*Vuli*). The overall classification accuracy for the land use maps of March, August, and October 2016 were 85.5%, 88.5%, and 91.6% with a kappa coefficient of 0.84, 0.87 and 0.91, respectively 150 (Msigwa et al., 2019). About 20 and 19 LULC classes in the Kikuletwa catchment were mapped for the wet and dry seasons, respectively. More details on the land use classes and their accuracies are found in Msigwa et al. (2019). The LULC maps were reclassified to match the SWAT land-use classification (see Table 3B in Appendix B). For instance, the SWAT land-use code 'PAST' was used to represent grazed grassland in the maps.

155 **2.3 Land-use Trajectories**

The LULC change trajectory methodology has been widely applied in many areas to assess LULC change and its impact on the environment. Researchers use trajectories to analyse the change happening between two images pixel by pixel (Mertens and Lambin, 2000; Swetnam, 2007; Zhou et al., 2008; Wang et al., 2012; Zomlot et al., 2017).

160 In this study, we extended the meaning of land-use trajectories from 'land-use change' to 'seasonal succession of land-use types for a given sample unit (pixel) with more than two observations at different times' (Zhou et al., 2008). We applied the method in this study to assess the agricultural seasonal dynamics for the meteorological dry and wet seasons of the Kikuletwa basin.

The land-use change trajectories were obtained by integrating three classified images to represent the
165 three cropping seasons so that pixel-based change trajectories could be found using GIS. A land-use
trajectory is the trajectory of a certain pixel in each of the three images. For example, a trajectory of
2→3→0 means for that pixel the land-use in March was rain-fed Maize (2), then in August, irrigated
mixed crop (3) and finally, in October, Bare land (0). This type of trajectory is classified as dynamic,
170 whereas a trajectory of 4→4→4 meaning the land-use is irrigated banana and coffee (4) in March, August,
and October, is a static trajectory. Thus, the LULC change trajectories were categorized into dynamic and
static land-use trajectories. We only implemented the trajectories from all agricultural land-uses except
irrigated banana and coffee and irrigated banana, maize and coffee land-uses which were combined as
irrigated banana and coffee land-use. About 74% of the trajectories were static while 26% of the
175 trajectories were dynamic. Figure 3 shows the spatial distribution of static and dynamic land-use
trajectories found in the study area. Only agricultural land-use and extensive agriculture LULC such as
grazed grassland and shrubland were considered when analysing the seasonal changes (dynamic land-
uses) and implemented in the SWAT+ model. We analyzed and implemented 40 land-use trajectories,
Appendix B, Table 1B shows few trajectories that were implemented.



Maps Data: Google Earth, ©2021, Image Landsat/Copernicus

Figure 3. Spatial distribution of main dynamic land-use trajectories and distinction between dynamic and static land-use identified in the study area.

Legend		
Id	Main Trajectory	Crop/ vegetation cover meaning
1	AGRL-BSVG-AGRL	Beans-space vegetation-beans
2	CORN-AGRL-PAST	Rainfed maize-beans-grassland
3	CORN-AGRL-BSVG	Rainfed maize-beans-space vegetation
4	AGRL-AGRL-BSVG	Irrigated mixed crops- irrigated mixed crops -space vegetation
5	CORN-AGRL-AGRL	Rainfed maize- Irrigated mixed crops - Irrigated mixed crops
6	AGRL-AGRL-AGRL	Irrigated mixed crops - Irrigated mixed crops - Irrigated mixed crops
7	AGRL-AGRL-PAST	Irrigated mixed crops - Irrigated mixed crops -grassland
8	AGRL-AGRL-PAST	Irrigated mixed crops - Irrigated mixed crops -grassland
9	SUGC-AGRL-AGRL	Irrigation sugarcane- Irrigated mixed crops - Irrigated mixed crops
10	AGRL-AGRL-AGRL	Irrigated mixed crops - Irrigated mixed crops - Irrigated mixed crops

2.4. SWAT+ Model

SWAT+ is a physically based, semi-distributed hydrological model and a restructured version of the Soil and Water Assessment Tool (SWAT) designed to face present and future challenges in water resources 185 modelling and management (Bieger et al., 2017). SWAT+ is more flexible in simulating the basin processes such as evapotranspiration, runoff, crop growth, nutrient, and sediment transport due to its watershed discretization and configuration. The HRUs are defined as a contiguous area, i.e., a representative field, with an associated user-defined length and width. The actual HRU is calculated based on the DEM, soil and land-use map inputs. Sub basins are delineated during the model construction, but 190 they are divided into water areas and one or more landscape units (LSU)(Bieger et al., 2017).

Land-use and management representation in SWAT+ can be done through the management file or using decision tables. Decision tables are an accurate yet compact way to model complex rule sets and their corresponding actions. Nkwasa et al. (2020) highlighted the greater flexibility provided by decision tables during the representation of agricultural practices in SWAT+. The model gives room for two or more 195 crops growing at the same time by defining the plant community in the specific plant file. The model enables the representation of the reality of cultivated tropical basins.

The ET in the model is estimated at HRU level. There are different methods (Priestley-Taylor, Penman-Monteith and Hargreaves) used to estimate ET in the SWAT+ model. More detailed information can be found in (Abiodun et al., 2017; Neitsch et al., 2002; Alemayehu et al., 2016). Our study adopted the 200 Hargreaves method (Hargreaves and Samani, 1982) to estimate ET due to the limited amount of input data such as solar radiation. The method has been tested in tropical basins such as the Mara basin linking Tanzania and Kenya (Alemayehu et al., 2016). Our aim was to use available ground data and not rely on remote sensing climate data such as solar radiation which is reported to have uncertainties (Alemayehu et al., 2016). SWAT model have also been successfully used in Pangani basin for different purposes 205 (Ndomba et al., 2008; Notter et al., 2012).

2.5 Land-use Trajectories Implementation in SWAT+

We combined three maps (March, August and October) to obtain the trajectory land-use map. Forty land-use trajectories were produced from the three seasonal land-use maps. These trajectories differ from the traditional approach as they not only use the agricultural statics but use land use maps to define the space. 210 Then each trajectory was assigned a SWAT+ land-use code (placeholder). For instance, a placeholder SWAT+ land-use code ‘MIXC’ signifies a CORN→TOMA→TOMA trajectory (rainfed maize to tomato to tomato land use trajectory) or ‘MIGS’ signifies a CORN →TOMA →BSVG trajectory (rainfed maize to tomato to sparse vegetation land use trajectory) as shown in Table 1B (Appendix B). A trajectory land-use map represented with the placeholder SWAT+ land-use codes using the lookup Table 1B (Appendix 215 B) for Kikuletwa basin was created. A python code (Appendix A) was used to assign trajectories of the placeholder SWAT+ land-use codes, and to create the trajectories’ management files i.e., ‘landuse.lum’, ‘management.sch’ and ‘hru-data.hru’ files. In the ‘Landuse.lum’ file, the trajectories were defined with respect to the plant community. ‘Management.sch’ file controls the timing of the planting and harvesting of the individual crops in the community (Table 1). For instance, the tomato and soya beans are planted 220 in the same field with different planting and harvesting schedule but grown at the same period. However, each crop was defined by its own plant community in new SWAT+ to make distinction between these crops. The ‘hru-data.hru’ file links the HRUs to the corresponding land-use management. The irrigation

schedules were implemented using decisions tables. The sources of irrigation water in the catchment was river and irrigation techniques were mostly furrow.

225 **Table 1.** An example of a ‘management.sch’ file input in dynamic SWAT+ model

name	numb_ops⁹	numb_auto¹⁰	op_typ¹¹	Mon¹²	Day¹³	hu_sch¹⁴	op_data1*	op_data2*	op_data3*
cor_agr_agr_m ¹	8	2	irr_toma_soy ²						
			irr_corn ²						
			plnt ³	3	15	0	corn ⁵	grain ⁸	0
			hvkl ⁴	8	15	0	corn	grain	1
			plnt	7	1	0	soyb ⁶	grain	2
agr_agr_agr_m ¹	8	2	plnt		20	0	toma	null	3
			hvkl	10	1	0	soyb	grain	4
			hvkl	10	20	0	toma ⁷	null	5
			plnt	10	30	0	corn	grain	6
			hvkl	2	28	0	corn	grain	7
			irr_toma_soy ²						
			irr_corn ²						
			plnt	3	15	0	soyb	grain	0
			hvkl	6	30	0	soyb	grain	1
			plnt	7	1	0	soyb	grain	2
			plnt	8	20	0	toma	null	3
			hvkl	10	1	0	soyb	grain	4
			hvkl	10	20	0	toma	null	5
			plnt	10	30	0	corn	grain	6
			hvkl	2	28	0	corn	grain	7

¹ name of the land-use management, ² points to the irrigation decision tables, ³ planting operation, ⁴ harvesting operation, ⁵ rainfed maize, ⁶ soy bean, ⁷ tomato, ⁸ harvest the grain portion of the crop, ⁹ number of operations, ¹⁰ number of auto-operations, ¹¹ operation type, ¹² month, ¹³ day, ¹⁴ heat unit schedule, * operations

230 **2.6 Model Configuration for both Static and Dynamic SWAT+ Models**

The SWAT+ model was setup using DEM, soil map and land-use map of March 2016 for the static representation scenario (static model) and using a trajectory map and files (described in section 2.5) for the dynamic representation scenario (dynamic Model). In the static model the crops were grown in the rain seasons from March till July and the land would be left bare. This is normally the case with most

235 SWAT model Application in SWAT (Ndomba et al., 2008; Gashaw et al., 2018; Koch et al., 2012). The same ground observations of rainfall and temperature were used (Appendix C, Table 1C) for both models. The precipitation stations were adjusted manually according to elevation and the potential maximum leaf area index of maize was adjusted to correspond to the field measurements of the basin. USDA Soil Conservation Service (SCS) curve number was used to estimate surface runoff and the muskingum
240 method used for channel routing.

For the static SWAT+ model, 23 sub-basins, 171 land scape units and 6086hru were generated with 14 land-use classes, while for the dynamic SWAT+ model, 23 sub-basins, 171 land scape units and 9333hru were generated with 40 land use classes representing the 40 different trajectories. The difference in the number of HRUs is related to the higher number of land-use classes in the dynamic land-use mapping.
245 The irrigation schedules were implemented through decisions tables (Arnold et al., 2018) by specifying a furrow irrigation method and using the rivers within the sub-basins as the source of irrigation. The model was run for a period of 8 years (2006 to 2013). The first two years were used as a warm up period.

2.7 Model Evaluation

Both the static and dynamic SWAT+ models were compared on how they simulate the water balance with specific focus on the ET component since this study aims at mainly improving the spatial distribution of blue and green water consumption. Hence, the SWAT+ models were not calibrated. The ET from both static and dynamic SWAT+ representation scenarios was compared with the remote sensing ET at a basin level for the same simulation period from 2008 to 2013. The remote sensing ET is an ensemble ET product from seven existing global scale ET products (IHE Delft, 2020). All the ET products are based on multi-spectral satellite measurements and surface energy balance models i.e. Global Land Evaporation Amsterdam Model (GLEAM) (Miralles et al., 2011), CSIRO MODIS Reflectance-based Evapotranspiration (CMRS-ET) (Guerschman et al., 2009), Operational Simplified Surface Energy Balance (SSEBop) (Senay et al., 2013), Atmosphere-Land Exchange Inverse Model (ALEXI) (Anderson et al., 2007), Surface Energy Balance System (SEBS) (Su, 2002), ETMonitor (Hu and Lia, 2015) and
255 MODIS Global Terrestrial Evapotranspiration Algorithm (MOD16) (Mu et al., 2011). The detailed
260

information on the ET products description and method are found in Hugo et al. (2019). The product was evaluated for the study area by comparing the basin water balance at three gauged stations; Karangai, Kikuletwa Power station and Tanzania Plantation Company (TPC) over a period of six years (2008-2013). The comparison of ET calculated using the water balance and remote sensing showed good agreement
265 (NSE= 0.77) for Kikuletwa Power station which covered 86% of the total basin area (Msigwa et al., 2019, 2021). Statistical metrics such as Nash-Sutcliffe efficiency (NSE), Root Mean Square Error (RMSE), Percent Bias (PBIAS) and adjusted R squared (R^2) were used to evaluate the both monthly ET from static and dynamic SWAT+ models against the remote sensing ET. Moreover, the Paired T-test statistical analysis was performed to find if there is significant difference between the ET from the static model and
270 that of dynamic model for only the dynamic land uses.

2.8 Estimating blue and green ET

The blue ET is a portion of crop evapotranspiration after application of irrigation while green ET is the evapotranspiration as a result of rainfall. The blue ET in this study was estimated as a difference between ET under irrigation and ET without irrigation (Liu and Yang, 2010). The SWAT+ dynamic land-use
275 implementation was run without irrigation and then later irrigation was applied. The green ET is the actual evapotranspiration from precipitation which can be kept in unsaturated soil and absorbed by plants and is then returned to the atmosphere via evapotranspiration. In this study, only the portion of blue water consumed from irrigation was considered and not all the blue water resources like other studies (Xie et al., 2020).

280 The SWAT+ model was run first assuming that no irrigation was carried out. The computed ET is called ET_{green} . Then the SWAT+ model was run again with irrigation being implemented and the ET computed is called ET_{total} as explained in the two scenarios below. ET_{blue} is computed by the difference of ET_{total} from the run with irrigation implantation and ET_{green} “Eq. (4)”.

The two scenarios to estimate blue ET

285 1. The seasonal dynamic SWAT+ is carried out by assuming the soil does not receive any irrigation water. The evapotranspiration computed using this first run is referred to as ET_{green}

2. The seasonal dynamic SWAT+ is carried out by assuming the soil receives sufficient irrigation water. The evapotranspiration computed using this second run is referred to as ET_{total}

Hence, ET_{blue} is computed from the “Eq. (4)” below

290 $ET_{blue} = ET_{total} - ET_{green}$ (4)

It should be noted that the trajectory implementation involves only two of the agricultural land-uses i.e. rainfed maize and mixed crop with exception of irrigated banana and coffee land-use and irrigated banana, coffee and maize land-use.

2.9 Comparison of SWAT+ results with other remote sensing methods

295 The SWAT+ blue and green ET were compared with the results from the four remote sensing data based methods namely: SN (Senay et al., 2016), EK (van Eekelen et al., 2015), Budyko method (Simons et al., 2020) and Soil Water Balance method -SWB (FAO and IHE Delft, 2019).

The SN method (Senay et al., 2016) is the simplest method whereby blue water is estimated as a difference between precipitation (P) and ET, followed by the modified method of van Eekelen et al., (2015) where 300 the effective fraction was introduced to reduce the amount of precipitation that evaporates. The Budyko method, as described in Simons et al., (2020), estimates green water from precipitation using an empirical relationship between actual evapotranspiration, precipitation and reference evapotranspiration. The Budyko equation, also called the Budyko curve, assumes a relationship between the evaporation ratio (ET/P) and climate aridity index (ET₀/P) to describe the water-energy balance for long term analysis.

305 The soil moisture balance model computes green (ET_{green}) and blue (ET_{blue}) water components of ET, by keeping track of the soil moisture balance and determining whether ET can be satisfied through direct precipitation and precipitation stored as soil moisture alone or if an additional water (surface or groundwater supply) is required. The study compares blue and green water estimations for all LULC classes for the Kikuletwa catchment.

3.1 Comparison of Simulated basin ET from Remote Sensing

Figure 4 shows the average monthly ET at the basin scale of Kikuletwa for the two model scenarios of SWAT+ and that from remote sensing. The dynamic SWAT+ model shows higher ET (by 20mm/month) matching the remote sensing pattern in the dry seasons (July to October) than the static SWAT+ model 315 implementation. This shows that there are agricultural activities occurring in the dry seasons. In the dynamic SWAT+ model, we implemented irrigated cropping during the dry seasons which led to an increase in ET.

The statistical analysis (Table 2) shows that both the SWAT+ simulations have a correlation (R^2) of above 0.5, when compared with monthly remote sensing ET. However, the monthly average ET value for the 320 dynamic land-use scenario is closer to the remote sensing ET, especially during the dry months from July to November where we implement more than one cropping season.

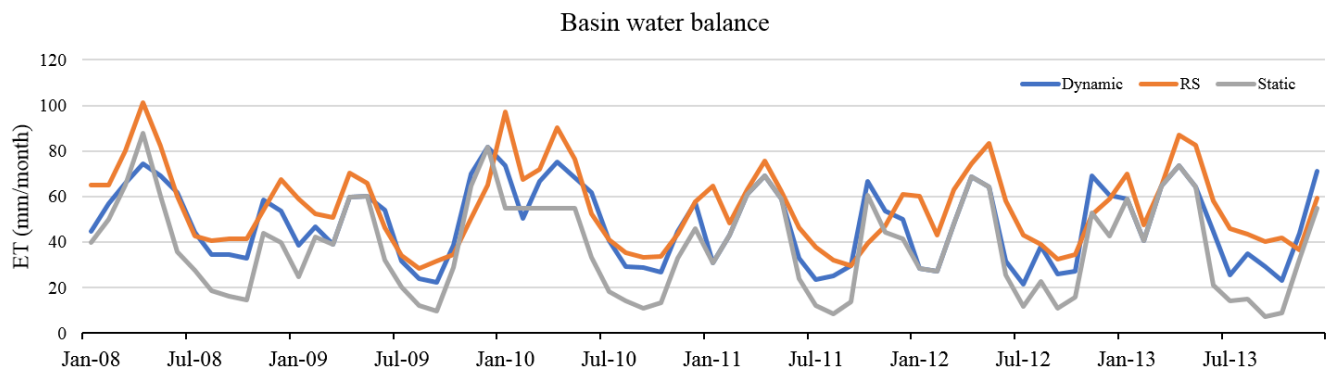
Unlike the commonly used static land-use scenario where only one cropping season was implemented per year, the monthly ET for the dynamic SWAT+ model implementation shows acceptable PBIAS of 13% whereas, the static SWAT+ model shows higher PBIAS of 30%. Moreover, the dynamic SWAT+ model 325 shows a good NSE of 0.4 while the static SWAT+ shows very low performance with an NSE of -0.46.

Table 3 shows the water balance component for the two scenarios. A notable difference is seen in ET increase (24%) and decrease in other water balance components (lateral flow; 27%, percolation; 42%, surface runoff; 32%). The mass balance (change in soil water balance) in percentage for the static SWAT+ model is higher (1.8%) than the dynamic SWAT+ model (0.5%). The most pronounced differences are 330 found when comparing the dynamic land-use representation on basin scale and the commonly used static land-use approach with remote sensing. Figure 5 shows the spatial distribution of ET from remote sensing, dynamic land-use and static land-use representation.

The average basin ET is 461mm/y, 573mm/y and 642 mm/y for the static SWAT+ model, dynamic SWAT+ model, and remote sensing, respectively. Generally, all the simulated ET from SWAT+ shows

335 lower annual average ET than remote sensing ET. However, the ET from static land-use representation shows a higher difference of 181mm/y whereas with the use of dynamic land-use, the difference in ET is only 69mm/y. The paired T-test results show that there is a significant difference between the ET from the static model and that of the dynamic model for the dynamic land-uses. A P value of 0.013 was obtained, which was less than the 0.05 confidence interval. Spatial distribution of ET from the SWAT+
340 models is different from remote sensing. However, visually, the spatial distribution of ET from the dynamic land-use scenario is closer and shows similar patches to remote sensing than the ET from the static land-use scenario (Figure 5).

345 The differences in ET spatial distribution (Figure 5) are vivid mostly in the trajectory implemented areas in the lowlands see Figure 3. Figure 6 shows the ET on the dynamic land-uses alone, the differences of the amount of the ET in these areas is more than 100mm per year. The vivid differences are seen on the right lower corner of the catchment where the differences in ET are more than 200mm/y. There are more areas with less than 400mm/y in the static model as compared to the dynamic model.



350 **Figure 4.** Average monthly ET for basin-scale summarized from remote sensing, dynamic land-use scenario and static land-use scenario.

Table 2. Statistical analysis of ET comparison of SWAT scenarios from Remote sensing

Statistic Parameter	Static SWAT+	Dynamic SWAT+
PBIAS	30%	13%
Nash-Sutcliffe efficiency (NSE)	-0.46	0.4
Adjusted R Square	0.6	0.6
RMSE (mm/month)	20.8	13.3

Table 3. Comparison of water balance component for the basin level

Water balance component (mm)	Static	Dynamic
Precipitation	814	814
Irrigation	0	8.25
Evapotranspiration	461	573
Lateral flow	139	101
Surface runoff	207	140
Percolation	21.7	12.6
%mass balance	1.8	0.53

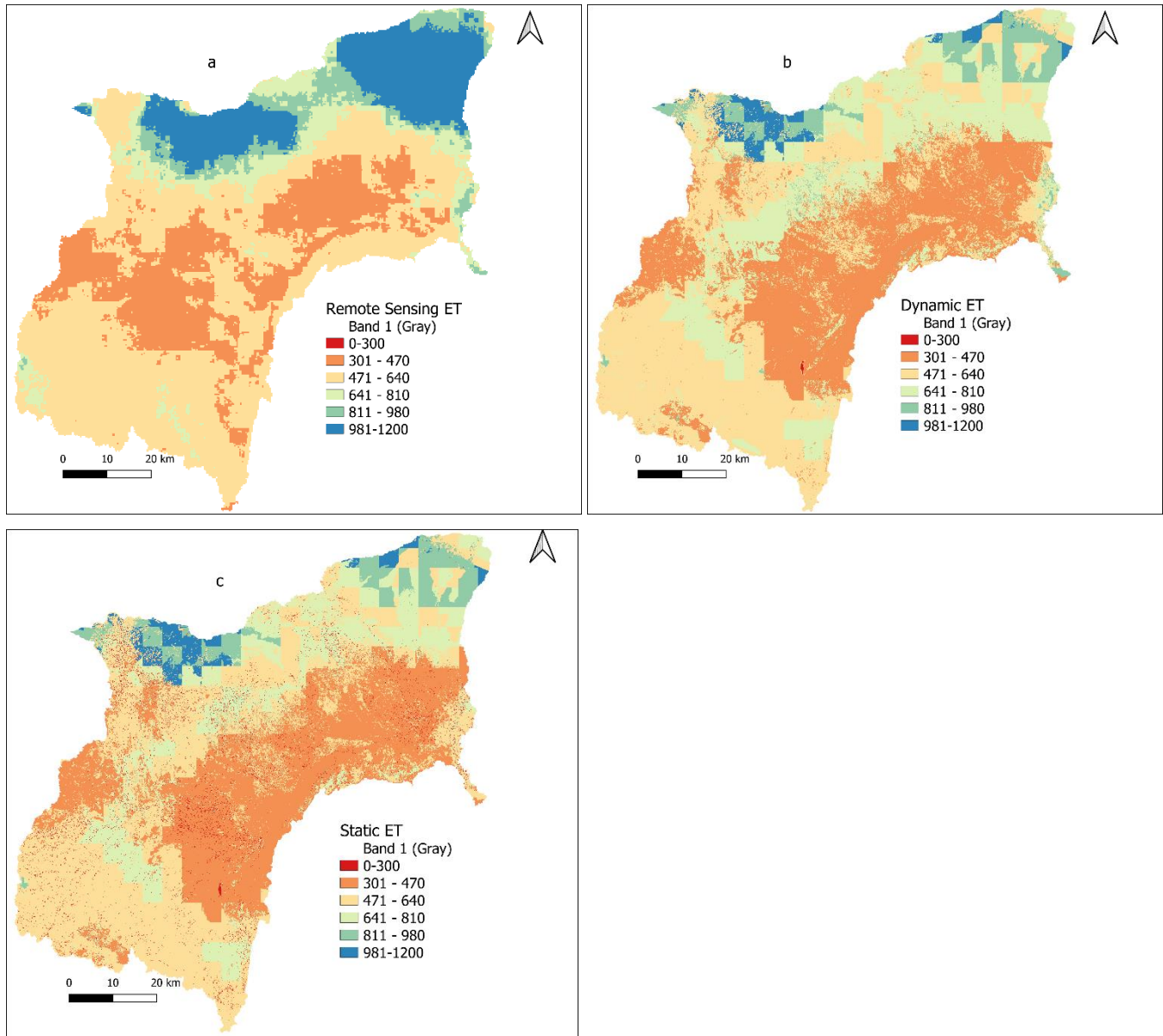


Figure 5. Spatial distribution of ET from a) Remote sensing b) dynamic land-use scenario and c) static

360 land-use scenario.

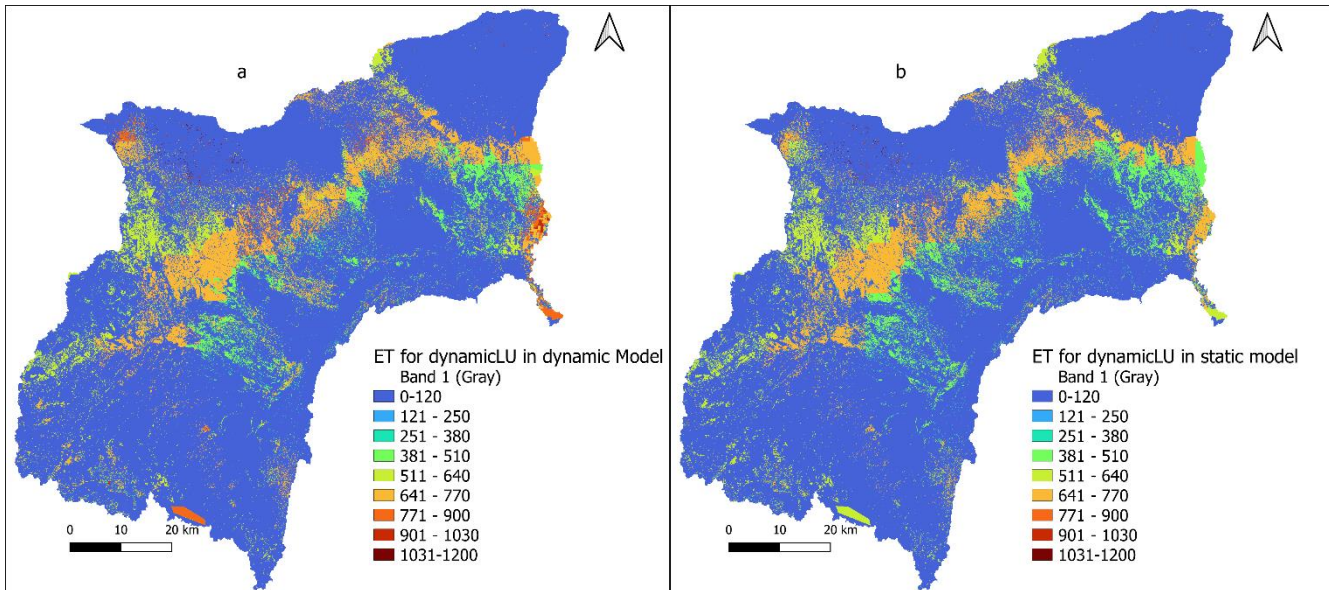
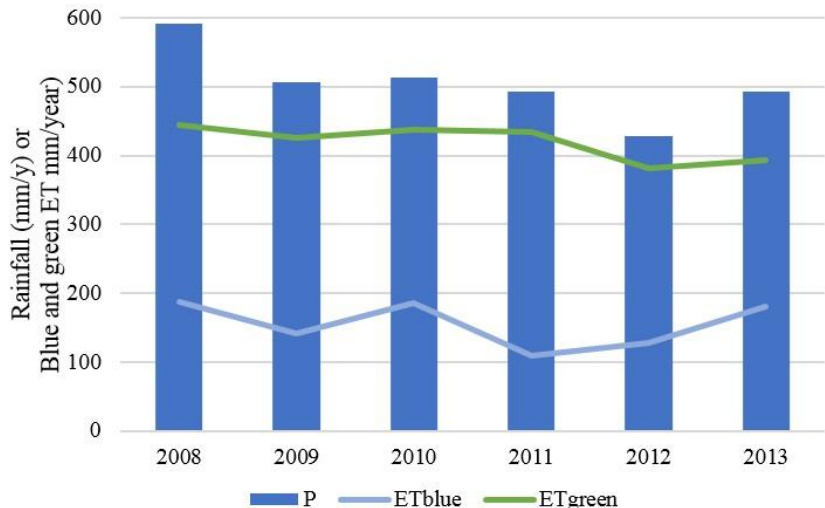


Figure 6. Spatial distribution of ET from dynamic Land-use for both a) dynamic and b) static SWAT+ Models.

3.2 Blue and Green ET

365 Figure 7 shows the trends of blue and green annual ET in the Kikuletwa basin for a period from 2008 to 2013. The implemented blue and green ET were mainly for irrigated mixed crop land-use due to implementation of trajectories. The annual average blue ET for irrigated mixed crops is 138mm which accounts for 25.5% of the annual average total ET and the annual average green ET is 402mm which accounts for 74.5% of the annual average total ET.



370

Figure 7. The annual variation of blue and green ET from 2008–2013.

Figure 8 shows that the spatial distribution of blue ET for agricultural areas in the Kikuletwa basin for implemented trajectories such as rainfed maize to tomato to irrigated maize land use trajectory (See Appendix 2, Table 2). The blue water is calculated from the irrigated implemented trajectories that mainly include irrigated mixed crops (soybeans, tomato and irrigated maize). Figure 8 shows that more than half of the total area consumes less than 200mm of blue ET. The higher blue ET is seen in the lower right corner where the irrigated sugarcane plantation is found.

375

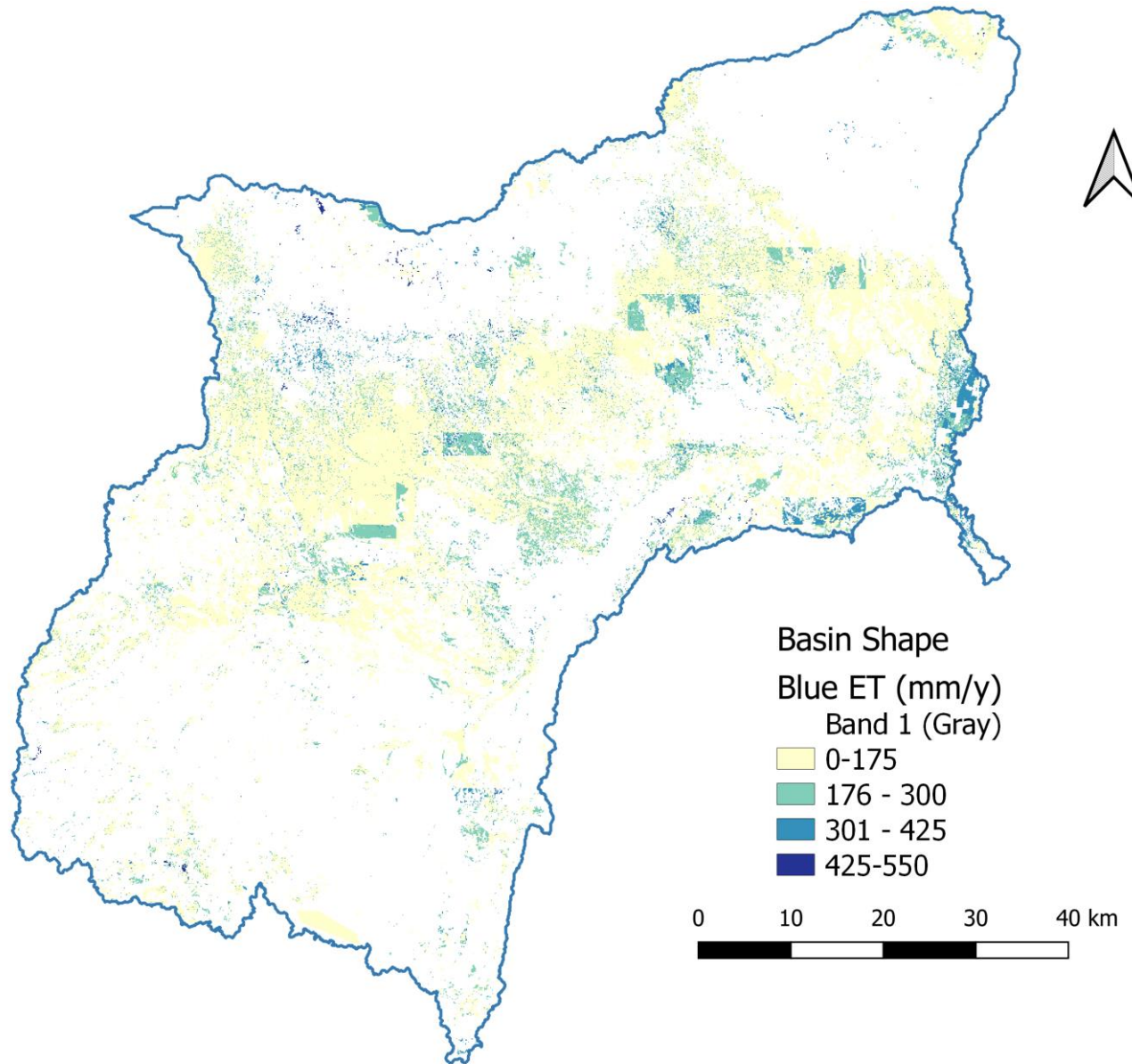


Figure 8. Spatial distribution of Blue ET for the implemented trajectories of rainfed and irrigated mixed crops land-use.

380

Figure 9 shows the comparison of average blue and green ET from four methods (Msigwa et al., 2021) with dynamic SWAT+. The value of both blue and green ET is closer to two methods, EK (van Eekelen) and SWB (Soil Water Balance) methods, which were indicated to have realistic values of blue and green

ET. Van Eekelen et al., (2015) is the method that analysed precipitation (P) and ET and applied an effective rainfall factor since not all rainfall will infiltrate and be stored in the unsaturated zone to be available for uptake by plants. Both ground data and remote sensing data could be used for data analysis-based approaches on an annual basis. The SWB model is a pixel by pixel vertical soil water balance model that splits green and blue ET by tracking of soil moisture balance and determining if the ET is satisfied only from rainfall or stored in the soil moisture or additional sources if required (FAO and IHE Delft, 390 2019).

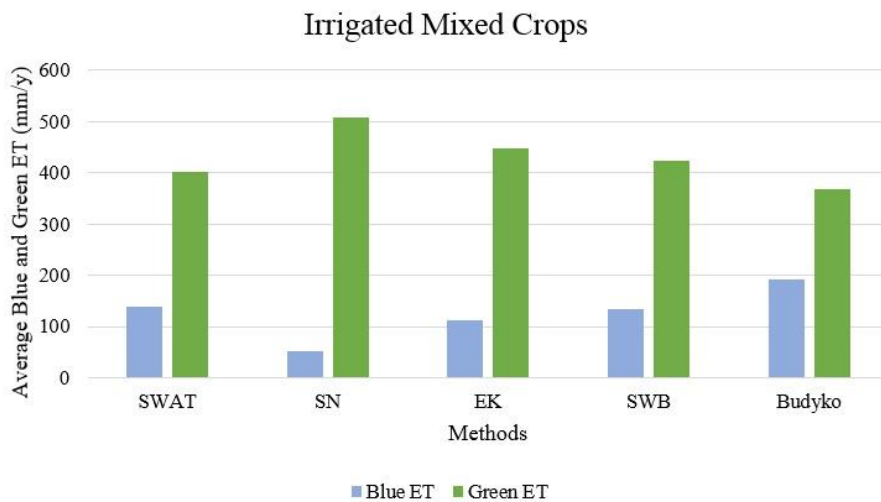


Figure 9. Blue and green ET comparison with other four methods from Msigwa et al. (2021).

4. Discussion

Some previous studies have represented annual land-use changes in SWAT and found that these have a 395 significant impact on hydrology (Wagner et al., 2016; Woldesenbet et al., 2017; Wagner et al., 2019). However, none of these studies has represented the seasonal dynamics of land use within a single year in a spatially distributed manner. Nkwasa et al. (2020) incorporated the seasonal land-use dynamic in SWAT and SWAT+ and found that models led to an improved vegetation simulation. This study did not show how the seasonal land-use dynamic improved water balance component such as ET. Our study uses of 400 agro-hydrological model (SWAT+) to represent blue and green ET for different cropping seasons

(represented by trajectory with time and space) and the use of remote sensing ET to evaluate the simulated ET from SWAT+. The study has compared a common default modelling approach where a static land-use map is used together with its management practices and a seasonal dynamic land-use representation where more than one cropping season is represented in a year. The spatial and temporal ET estimates 405 from two model setups were compared with remote sensing ET. An increase of 112mm/y of the ET is seen when seasonal dynamic land-use is implemented in the dynamic model to match the remote sensing ET as compared to when a static land-use map is used in the static model. The ET results from the dynamic model are significantly different from the ET in the static model for the dynamic land-use. The models show differences in water balance components, this is due to implementation of the land-use trajectory in 410 the dynamic model.

A remarkable difference is seen in the spatial distribution of ET from static and dynamic land-use SWAT+ representation. The dynamic land-use SWAT+ visually is similar to a remote sensing map compared to the static land-use SWAT+. This is because of the added management practices such as irrigated cropping in the dry seasons, unlike the default SWAT+ with a static land use throughout the simulation period. The 415 ET from dynamic land-use setup could not reach maximum satellite ET because the satellite ET estimates also have uncertainties in the mountainous areas because of the presence of cloud cover. Moreover, different methods for estimating ET could lead to these differences. Climate ground stations (temperature, wind speed, relative humidity and solar radiation) were used for ET simulation in SWAT+ model while the remote sensing use the energy balance models, mostly remote sensing data.

420 On the other hand, the ET from the static land cover such as forest from the static and dynamic model setup show different ET values this could be because of the difference in the initial model setup. The model setup for static used a March land use map with only 14 land use classes, while the dynamic model used a land use map with 40 trajectories. Hence, the changes in the ET might be due to the different land use maps yielding different number of HRUs. In order to avoid such difference, one could have a initial 425 setup with same land uses then trajectory implementation could only be with the agricultural land use

Furthermore, the ET estimates from the dynamic SWAT+ model were used to estimate blue and green ET. The blue and green ET estimates from SWAT+ for the mixed crop land-use show no significant difference in the values from the two methods (EK and SWB) assessed in the (Msigwa et al., 2021).

These findings demonstrate the importance of the representation of seasonal land-use dynamic in 430 modelling blue and green water consumption. Normally, most models use NDVI to represent seasonal changes (Amri et al., 2011; Ferreira et al., 2003), whereas the use of dynamic land-use leads to improved accuracy of seasonal simulations of the water uses (Nkwasa et al., 2020). Seasonal land-use maps can add information on management practices of changes in temporal crop rotation and irrigation water use at a 435 spatial scale. However, to account for accurate seasonality of land-use, more than 3 maps within a year should be represented, ideally 12 maps each year. This would enable a more complete understanding of the agricultural land-use classes and minimize errors in the trajectory analysis. However, Landsat 8 is associated with cloud most especially in the rainy season. Cloud masking techniques is needed before further analysis of the images. Also, there were uncertainties associated with the trajectories for example unrealistic trajectories like change from crop to forest then crop again. These types of trajectories were 440 corrected and reclassified.

The Landsat 8 images used in this study to map seasonal land-use dynamics did not have a revisit time (16-day) that is small enough to acquire an adequate number of monthly images to represent the year. More products are now becoming available (Sentinel-2, 5-day revisit time) that have a higher temporal resolution, which would aid in the collection of more cloud free images to represent seasonality within 445 the year.

Although it appears important to include seasonal land use dynamic, one may claim that the annual land-use implementation is enough when studying the effect of land use in hydrology. Our study shows a significant impact of the representation of seasonal land-use in the SWAT+ model by reducing the errors in water consumption estimations.

450 **5. Conclusion**

Understanding of the spatial-temporal variability of agricultural water consumption in terms of blue water, requires accurate estimates of ET. This study has demonstrated the importance of incorporating seasonal land-use dynamic to improve simulated ET for further blue and green ET estimates using a SWAT+ model. Although the static representation gives equally reasonable good R^2 results of more than 455 0.5, we found out that the RMSE for the static model result is significantly higher as compared to the RMSE of the dynamic model result by about 112 mm per year. Moreover, the ET from the dynamic SWAT+ model gave a low PBIAS (13%) and a relatively good NSE of 0.4 compared to the ET from static SWAT+ that gives a higher PBIAS (20.8%) and a negative NSE of -0.46. The study showed that a 460 dynamic land use representation in the SWAT+ model gave ET estimates closer to the remote sensing ET as compared to the default model with a static land-use representation. The improved ET map from the dynamic SWAT+ model improved the blue ET estimates as compared to use of static ET maps that does not implement irrigation in dry season. Hence, estimated blue ET correspond to the blue ET amount of past study in the basin (Msigwa et al., 2021). It is concluded that the representation of seasonal land use dynamics is essential to correctly simulate the agricultural (blue and green) water consumption. Also, for 465 land use change studies, it is important to correctly represent the seasonal land use dynamics.

References

Abiodun, O. O., Guan, H., Post, V. E. A., and Batelaan, O.: Comparison of MODIS and SWAT Evapotranspiration over a Complex Terrain at Different Spatial Scales, *Hydrol. Earth Syst. Sci. Discuss.*, 1–36, <https://doi.org/10.5194/hess-2017-599>, 2017.

470 Alemayehu, T., van Griensven, A., and Bauwens, W.: Evaluating CFSR and WATCH data as input to SWAT for the estimation of the potential evapotranspiration in a data-scarce Eastern-African catchment, *J. Hydrol. Eng.*, 21, 1–16, [https://doi.org/10.1061/\(ASCE\)HE.1943-5584.0001305](https://doi.org/10.1061/(ASCE)HE.1943-5584.0001305), 2016.

Amri, R., Zribi, M., Lili-Chabaane, Z., Duchemin, B., Gruhier, C., and Chehbouni, A.: Analysis of vegetation behavior in a North African semi-arid region, Using SPOT-VEGETATION NDVI data, *Remote Sens.*, 3, 2568–2590, 475 <https://doi.org/10.3390/rs3122568>, 2011.

Anderson, J. R., Hardy, E. E., Roach, J. T., Witmer, R. E., Anderson, B. J. R., Hardy, E. E., Roach, J. T., and Witmer, R. E.: A land use and land cover classification system for use with remote sensor data, 1976.

Anderson, M. C., Norman, J. M., Mecikalski, J. R., Otkin, J. A., and Kustas, W. P.: A climatological study of

evapotranspiration and moisture stress across the continental United States based on thermal remote sensing : 2 . Surface
480 moisture climatology, *J. Geophys. Res.*, 112, 1–13, <https://doi.org/10.1029/2006JD007507>, 2007.

Arnold, J. G., Bieger, K., White, M. J., Srinivasan, R., Dunbar, J. A., and Allen, P. M.: Use of decision tables to simulate
management in SWAT+, 10, 1–10, <https://doi.org/10.3390/w10060713>, 2018.

Bieger, K., Arnold, J. G., Rathjens, H., White, M. J., Bosch, D. D., Allen, P. M., Volk, M., and Srinivasan, R.: Introduction to
SWAT+, A Completely Restructured Version of the Soil and Water Assessment Tool, *J. Am. Water Resour. Assoc.*, 53, 115–
485 130, <https://doi.org/10.1111/1752-1688.12482>, 2017.

van Eekelen, M. W., Bastiaanssen, W. G. M., Jarmain, C., Jackson, B., Ferreira, F., van der Zaag, P., Saraiva Okello, A.,
Bosch, J., Dye, P., Bastidas-Obando, E., Dost, R. J. J., and Luxemburg, W. M. J.: A novel approach to estimate direct and
indirect water withdrawals from satellite measurements: A case study from the Incomati basin, *Agric. Ecosyst. Environ.*, 200,
126–142, <https://doi.org/10.1016/j.agee.2014.10.023>, 2015.

490 Falkenmark, M. and Rockström, J.: The new blue and green water paradigm: Breaking new ground for water resources
planning and management, *J. Water Resour. Plan. Manag.*, 132, 129–132, [https://doi.org/10.1061/\(ASCE\)0733-9496\(2006\)132:3\(129\)](https://doi.org/10.1061/(ASCE)0733-
9496(2006)132:3(129)), 2006.

FAO and IHE Delft: Water Accounting in the Litani River Basin-Remote sensing for water productivity, Water accounting
series, Rome, 2019.

495 Feng, H., Zhao, X., Chen, F., and Wu, L.: Using land use change trajectories to quantify the effects of urbanization on urban
heat island, *Adv. Sp. Res.*, 53, 463–473, <https://doi.org/10.1016/j.asr.2013.11.028>, 2014.

Ferreira, L. G., Yoshioka, H., Huete, A., and Sano, E. E.: Seasonal landscape and spectral vegetation index dynamics in the
Brazilian Cerrado: An analysis within the Large-Scale Biosphere-Atmosphere Experiment in Amaz??nia (LBA), *Remote Sens.
Environ.*, 87, 534–550, <https://doi.org/10.1016/j.rse.2002.09.003>, 2003.

500 Gao, J., Sheshukov, A. Y., Yen, H., Kastens, J. H., and Peterson, D. L.: Impacts of incorporating dominant crop rotation
patterns as primary land use change on hydrologic model performance, *Agric. Ecosyst. Environ.*, 247, 33–42,
<https://doi.org/10.1016/j.agee.2017.06.019>, 2017.

Gashaw, T., Tulu, T., Argaw, M., and Worqlul, A. W.: Modeling the hydrological impacts of land use/land cover changes in
the Andassa watershed, Blue Nile Basin, Ethiopia, *Sci. Total Environ.*, 619–620, 1394–1408,
505 <https://doi.org/10.1016/j.scitotenv.2017.11.191>, 2018.

Glavan, M. ˇ, Pintar, M., and Urbanc, J.: Spatial variation of crop rotations and their impacts on provisioning ecosystem
services on the river Drava alluvial plain Sustainability of Water Quality and Ecology Spatial variation of crop rotations and
their impacts on provisioning ecosystem services, *Sustain. Water Qual. Ecol.*, <https://doi.org/10.1016/j.swaqe.2015.01.004>,
2015.

510 van Griensven, A., Ndomba, P., Yalew, S., and Kilonzo, F.: Critical review of SWAT applications in the upper Nile basin
countries, *Hydrol. Earth Syst. Sci.*, 16, 3371–3381, <https://doi.org/10.5194/hess-16-3371-2012>, 2012.

Guerschman, J. P., Van Dijk, A. I. J. M., Mattersdorf, G., Beringer, J., Hutley, L. B., Leuning, R., Pipunic, R. C., and Sherman,

B. S.: Scaling of potential evapotranspiration with MODIS data reproduces flux observations and catchment water balance observations across Australia, *J. Hydrol.*, 369, 107–119, <https://doi.org/10.1016/j.jhydrol.2009.02.013>, 2009.

515 Hargreaves, G. H. and Samani, Z. A.: Estimating potential evapotranspiration, *J. Irrig. Drain. Eng.*, 108, 225–230, 1982.

Hengl, T., Heuvelink, G. B. M., Kempen, B., Leenaars, J. G. B., Walsh, M. G., Shepherd, K. D., Sila, A., MacMillan, R. A., De Jesus, J. M., Tamene, L., and Tondoh, J. E.: Mapping soil properties of Africa at 250 m resolution: Random forests significantly improve current predictions, *PLoS One*, 10, 1–26, <https://doi.org/10.1371/journal.pone.0125814>, 2015.

Hoekstra, A. Y.: Green-blue water accounting in a soil water balance, *Adv. Water Resour.*, 129, 112–117, 520 <https://doi.org/10.1016/j.advwatres.2019.05.012>, 2019.

Hu, G. and Lia, L.: Monitoring of evapotranspiration in a semi-arid inland river basin by combining microwave and optical remote sensing observations, *Remote Sens.*, 7, 3056–3087, <https://doi.org/https://doi.org/10.3390/rs70303056>, 2015.

Hugo, V., Espinoza-dávalos, G. E., Hessels, T. M., Moreira, D. M., Comair, G. F., and Bastiaanssen, W. G. M.: The spatial variability of actual evapotranspiration across the Amazon River Basin based on remote sensing products validated with flux 525 towers, *Ecol. Process. Process.*, 8, 2019.

IHE Delft: ET Ensemble Version 1.0 (ETensV1.0) Technical Documentation, 2020.

Jain, M., Mondal, P., Defries, R. S., Small, C., and Galford, G. L.: Remote Sensing of Environment Mapping cropping intensity of smallholder farms: A comparison of methods using multiple sensors, *Remote Sens. Environ.*, 134, 210–223, 530 <https://doi.org/10.1016/j.rse.2013.02.029>, 2013.

Jeyrani, F., Morid, S., and Srinivasan, R.: Assessing basin blue–green available water components under different management and climate scenarios using SWAT, *Agric. Water Manag.*, 256, 107074, <https://doi.org/10.1016/j.agwat.2021.107074>, 2021.

Koch, F. J., Van Griensven, A., Uhlenbrook, S., Tekleab, S., and Teferi, E.: The effects of land use change on hydrological responses in the Choke Mountain Range (Ethiopia) - A new approach addressing land use dynamics in the model SWAT, *iEMSSs 2012 - Manag. Resour. a Ltd. Planet Proc. 6th Bienn. Meet. Int. Environ. Model. Softw. Soc.*, 3022–3029, 2012.

535 Liang, J., Liu, Q., Zhang, H., Li, X., Qian, Z., Lei, M., Li, X., Peng, Y., Li, S., and Zeng, G.: Interactive effects of climate variability and human activities on blue and green water scarcity in rapidly developing watershed, *J. Clean. Prod.*, 265, 121834, <https://doi.org/10.1016/j.jclepro.2020.121834>, 2020.

Liu, J. and Yang, H.: Spatially explicit assessment of global consumptive water uses in cropland: Green and blue water, *J. Hydrol.*, 384, 187–197, <https://doi.org/10.1016/j.jhydrol.2009.11.024>, 2010.

540 Mertens, B. and Lambin, E. F.: Land-Cover-Change Trajectories in Southern Cameroon, *Ann. Assoc. Am. Geogr.*, 90, 467–494, <https://doi.org/10.1111/0004-5608.00205>, 2000.

Miralles, D. G., Holmes, T. R. H., De Jeu, R. A. M., Gash, J. H., Meesters, A. G. C. A., and Dolman, A. J.: Global land-surface evaporation estimated from satellite-based observations, *Hydrol. Earth Syst. Sci.*, 15, 453–469, <https://doi.org/10.5194/hess-15-453-2011>, 2011.

545 Msigwa, A., Komakech, H. C., Verbeiren, B., Salvadore, E., Hessels, T., Weerasinghe, I., and van Griensven, A.: Accounting for seasonal land use dynamics to improve estimation of agricultural irrigation water withdrawals, 11,

https://doi.org/10.3390/w11122471, 2019.

Msigwa, A., Komakech, H. C., Salvadore, E., Seyoum, S., Mul, M. L., and Griensven, A. Van: Comparison of blue and green water fluxes for different land use classes in a semi-arid cultivated catchment using remote sensing, *J. Hydrol. Reg. Stud.*, 36, 100860, https://doi.org/10.1016/j.ejrh.2021.100860, 2021.

550 Mu, Q., Zhao, M., and Running, S. W.: Improvements to a MODIS global terrestrial evapotranspiration algorithm, *Remote Sens. Environ.*, 115, 1781–1800, https://doi.org/10.1016/j.rse.2011.02.019, 2011.

Ndomba, P., Mtalo, F., and Killingtveit, A.: SWAT model application in a data scarce tropical complex catchment in Tanzania, *Phys. Chem. Earth*, 33, 626–632, https://doi.org/10.1016/j.pce.2008.06.013, 2008.

555 Neitsch, S. L., Arnold, J. G., Kiniry, J. R., Srinivasan, R., and Williams, J. R.: Soil and Water Assessment Tool—User’s Manual 2002, TWRI Report TR-192, 412 pp., 2002.

Nkwasa, A., Chawanda, C. J., Msigwa, A., Komakech, H. C., Verbeiren, B., and van Griensven, A.: How can we represent seasonal land use dynamics in SWAT and SWAT+ models for African cultivated catchments, 12, 1–19, https://doi.org/10.3390/W12061541, 2020.

560 Notter, B., Hurni, H., Wiesmann, U., and Abbaspour, K. C.: Modelling water provision as an ecosystem service in a large East African river basin, *Hydrol. Earth Syst. Sci.*, 16, 69–86, https://doi.org/10.5194/hess-16-69-2012, 2012.

Schuol, J., Abbaspour, K. C., Yang, H., Srinivasan, R., and Zehnder, A. J. B.: Modeling blue and green water availability in Africa, *Water Resour. Res.*, 44, 1–18, https://doi.org/10.1029/2007WR006609, 2008.

565 Senay, G. B., Bohms, S., Singh, R. K., Gowda, P. H., Velpuri, N. M., Alemu, H., and Verdin, J. P.: Operational Evapotranspiration Mapping Using Remote Sensing and Weather Datasets: A New Parameterization for the SSEB Approach, *J. Am. Water Resour. Assoc.*, 49, 577–591, https://doi.org/10.1111/jawr.12057, 2013.

Senay, G. B., Friedrichs, M., Singh, R. K., Manohar, N., Velpuri, N. M., and Manohar, N.: Evaluating Landsat 8 evapotranspiration for water use mapping in the Colorado River Basin, *Remote Sens. Environ.*, 185, 171–185, https://doi.org/10.1016/j.rse.2015.12.043, 2016.

570 Serur, A. B.: Modeling blue and green water resources availability at the basin and sub-basin level under changing climate in the Weyb River basin in Ethiopia, *Sci. African*, 7, e00299, https://doi.org/10.1016/j.sciaf.2020.e00299, 2020.

Su, Z.: The Surface Energy Balance System (SEBS) for estimation of turbulent heat fluxes To cite this version : HAL Id : hal-00304651 The Surface Energy Balance System (SEBS) for estimation of turbulent heat fluxes, *Hydrol. Earth Syst. Sci. Discuss.*, 6, 85–100, 2002.

575 Swetnam, R. D.: Rural land use in England and Wales between 1930 and 1998: Mapping trajectories of change with a high resolution spatio-temporal dataset, *Landsc. Urban Plan.*, 81, 91–103, https://doi.org/10.1016/j.landurbplan.2006.10.013, 2007.

Velpuri, N. M. and Senay, G. B.: Partitioning Evapotranspiration into Green and Blue Water Sources in the Conterminous United States, *Scientific Reports*, Springer US, 1–12 pp., https://doi.org/10.1038/s41598-017-06359-w, 2017.

580 Wagner, P. D., Bhallamudi, S. M., Narasimhan, B., Kantakumar, L. N., Sudheer, K. P., Kumar, S., Schneider, K., and Fiener, P.: Dynamic integration of land use changes in a hydrologic assessment of a rapidly developing Indian catchment, *Sci. Total*

Environ., 539, 153–164, <https://doi.org/10.1016/j.scitotenv.2015.08.148>, 2016.

Wagner, P. D., Bhallamudi, S. M., Narasimhan, B., Kumar, S., Fohrer, N., and Fiener, P.: Comparing the effects of dynamic versus static representations of land use change in hydrologic impact assessments, Environ. Model. Softw., 122, 1–9, <https://doi.org/10.1016/j.envsoft.2017.06.023>, 2019.

585 Wang, D., Gong, J., Chen, L., Zhang, L., Song, Y., and Yue, Y.: Spatio-temporal pattern analysis of land use/cover change trajectories in Xihe watershed, Int. J. Appl. Earth Obs. Geoinf., 14, 12–21, <https://doi.org/10.1016/j.jag.2011.08.007>, 2012.

Woldesenbet, T. A., Elagib, N. A., Ribbe, L., and Heinrich, J.: Hydrological responses to land use/cover changes in the source region of the Upper Blue Nile Basin, Ethiopia, Sci. Total Environ., 575, 724–741, <https://doi.org/10.1016/j.scitotenv.2016.09.124>, 2017.

590 Xie, P., Zhuo, L., Yang, X., Huang, H., Gao, X., and Wu, P.: Spatial-temporal variations in blue and green water resources , water footprints and water scarcities in a large river basin: A case for the Yellow River basin, J. Hydrol., 590, 125222, <https://doi.org/10.1016/j.jhydrol.2020.125222>, 2020.

Zhou, Q., Li, B., and Kurban, A.: Trajectory analysis of land cover change in arid environment of China, Int. J. Remote Sens., 29, 1093–1107, <https://doi.org/10.1080/01431160701355256>, 2008.

595 Zomlot, Z., Verbeiren, B., Huysmans, M., and Batelaan, O.: Trajectory analysis of land use and land cover maps to improve spatial-temporal patterns, and impact assessment on groundwater recharge, J. Hydrol., <https://doi.org/10.1016/j.jhydrol.2017.09.032>, 2017.

Appendices

600 Appendix A. Make Management Script

```

import sys
from PIL import Image
import numpy as np

605 def open_tif_as_array(tif_file):
    im = Image.open(tif_file)
    imarray = np.array(im)
    return imarray

610 def empty_line():
    print("")

def write_to(filename, text_to_write, report = False):
    """
    615     a function to write to file
    """

```

```

g = open(filename, 'w')
try:
    g.write(text_to_write)
    if report:
        print('\n\t> file saved to ' + filename)
except:
    print("\t> error writing to {0}, make sure the file is not open in another program"
900
.format(
    filename)
    response = input("\t> continue? (Y/N): ")
    if response == "N" or response == "n":
        sys.exit()
g.close
910
def show_progress(count, end_val, string_before = "percent complete", string_after = "", ba
r_length = 30):
    percent = float(count) / end_val
    hashes = "#" * int(round(percent * bar_length))
915
    spaces = ' ' * (bar_length - len(hashes))
    sys.stdout.write("\r{str_b} [{bar}] {pct}% {str_after}\t\t".format(
        str_b = string_before,
        bar = hashes + spaces,
        pct = '{0:.2f}'.format(percent * 100),
        str_after = string_after))
920
    sys.stdout.flush()

def read_from(filename):
    """
    a function to read ascii files
    """
    try:
        g = open(filename, 'r')
    except:
        print("\t> error reading {0}, make sure the file exists".format(filename))
        return
930
    file_text = g.readlines()
    g.close
    return file_text
935
class schedule_data:
    def __init__(self, crop_name):
        self.crop_name = crop_name
        self.oct_plant = ""
940
        self.oct_harvest = ""
        self.aug_plant = ""
        self.aug_harvest = ""
        self.mar_plant = ""
        self.mar_harvest = ""

```

```

665
base_txt = "C:/Users/james/Desktop/root/anna/new/new_swat_plus_model/kikuletwa/Scenarios/De
fault/TxtInOut"
inputs_path = "trajectory_files"

670 # read trajectory data
trajectories = open_tif_as_array("{base}/{fn}".format(base = inputs_path, fn = "trajectory_
map_thres.tif"))
legend_raw = read_from("{base}/{fn}".format(base = inputs_path, fn = "trajectory_lookup_fn
al.csv"))
675 dates_raw = read_from("{base}/{fn}".format(base = inputs_path, fn = "crop_plant_harvest.csv
"))

landuse_lum_raw = """landuse.lum: created for trajectories
680 name cal_group plnt_com mgt cn
2 cons_prac urban urb_ro ov_mann tile
sep vfs grww bmp
"""
plant_ini_raw = """plant.ini: created for trajectories
685 pcom_name plt_cnt rot_yr_ini plt_name lc_status lai_init bm_init
phu_init plnt_pop yrs_init rsd_init
"""

management_raw = """management.sch: created for trajectories
690 name numb_ops numb_auto op_typ mon day
hu_sch op_data1 op_data2 op_data3
"""

landuse_lum = landuse_lum_raw
plant_ini = plant_ini_raw
695

trajectories_dictionary = {}
# trajectory_hru_lum_dict = {}
crop_schedule_dictionary = {}
month_dictionary = {'None': "None", "Jan": "1", "Feb": "2", "Mar": "3", "Apr": "4", "May": "5",
700 "Jun": "6", "Jul": "7", "Aug": "8", "Sep": "9", "Oct": "10", "Nov": "11", "Dec": "12"}

for line in dates_raw[1:]:
    parts = line.split(",")
    crop_schedule_dictionary[parts[0].lower()] = schedule_data(parts[0])
    crop_schedule_dictionary[parts[0].lower()].oct_plant = "{0}".format(parts[5]).strip("\n
")
    crop_schedule_dictionary[parts[0].lower()].oct_harvest = "{0}".format(parts[6]).strip("
\n")
    crop_schedule_dictionary[parts[0].lower()].aug_plant = "{0}".format(parts[3]).strip("
\n")
710 ")", crop_schedule_dictionary[parts[0].lower()].aug_harvest = "{0}".format(parts[4]).strip("
\n")

```

```

        crop_schedule_dictionary[parts[0].lower()].mar_plant = "{0}".format(parts[1]).strip("\n")
715    crop_schedule_dictionary[parts[0].lower()].mar_harvest = "{0}".format(parts[2]).strip("\n")
    for line in legend_raw[1:]:
        trajectories_dictionary[line.split(",")[1].lower()] = line.split(",")[2].strip("\n").l0
720    wer()

growing_list = ["FRST", "BANA", "SHRB", "SUGC"]

for crop_name in trajectories_dictionary:
725    # create lum
    parts = trajectories_dictionary[crop_name].split("-")
    com_mgt_prefix = "{0}_{1}_{2}".format(parts[0][:3], parts[1][:3], parts[2][:3])
    com_mgt_prefix = com_mgt_prefix.lower()
    if True: #not ((parts[0] == parts[1]) and (parts[0] == parts[2])):
730        line_ = "{lum_t}           null           {plt_comm} {mgt}           rc_strow_g
        cross_slope           null           null   convtill_nores           null
        null           null           null           null   \n".format(
            lum_t = trajectories_dictionary[crop_name].lower().replace("-", "_"),
            plt_comm = "{0}_c".format(com_mgt_prefix),
535        mgt = "{0}_m".format(com_mgt_prefix),
        )
        landuse_lum += line_
        # print(trajectories_dictionary[crop_name])

740    # create comm
    comm_ = "{comm_n}_c           //no           1 \n".format(comm_n = com_mgt_prefix)
    plt_count = 0
    done = []
    for plt in parts:
745        if plt == "AGRL":
            for agrl_crop in ["TOMA", "CORN", "SOYB"]:
                if not agrl_crop.lower() in done:
                    if plt in growing_list:
                        grow_ini = "y"
                    else:
                        grow_ini = "n"
                    plt_count += 1
                    comm_ += "
{growing}      0.00000      0.00000      0.00000      0.00000      {agrl_crop}
755 .00000 \n".format(agrl_crop = agrl_crop.lower(), growing = grow_ini)
                    done.append(agrl_crop)

                    continue

760        if not plt.lower() in done:
            if plt in growing_list:

```

```

    grow_ini = "y"
  else:
    grow_ini = "n"
  plt_count += 1
  comm__ += "
}      0.00000      0.00000      0.00000      0.00000      {plt_1}      {growing
format(plt_1 = plt.lower(), growing = grow_ini)
done.append(plt)

770
  comm__ = comm__.replace("//no", str(plt_count))
  plant_ini += comm__

# create_management
775
schedule_name = "{0}_m".format(com_mgt_prefix)
number_of_manual_ops = 0
number_of_auto_ops = 0

done_2 = []
780
  management_section_head = "{mgt_name}"                                {number_manual}
{number_auto}
  management_section_body = ""
  counter_mgt = 0
785
  for plant_index in range(0, 3):

    date_day_plant = None
    date_mnt_plant = None
790
    date_day_harvest = None
    date_mnt_harvest = None
    agrl_list = []

    if plant_index == 0:
      agrl_list = ["soyb"]

    if plant_index == 1:
      agrl_list = ["soyb", "toma"]
800
    if plant_index == 2:
      agrl_list = ["corn"]

    if parts[plant_index] == "agrl":
      for agrl_crop_mgt in agrl_list:
        if plant_index == 0:
          date_day_plant = crop_schedule_dictionary[agrl_crop_mgt].mar_plant.spli
805
t("-")[0]

```

```

810  t("-")[-1]
        date_mnt_plant = crop_schedule_dictionary[agrl_crop_mgt].mar_plant.split()
        if plant_index == 1:
            date_day_plant = crop_schedule_dictionary[agrl_crop_mgt].aug_plant.split()
            date_mnt_plant = crop_schedule_dictionary[agrl_crop_mgt].aug_plant.split()
815  t("-")[-1]
        if plant_index == 2:
            date_day_plant = crop_schedule_dictionary[agrl_crop_mgt].oct_plant.split()
            date_mnt_plant = crop_schedule_dictionary[agrl_crop_mgt].oct_plant.split()
820  t("-")[-1]
            management_body_line = ""
            {activity}{mnt}{day}      0.00000           {crp}           null      {ord
er}.00000  ".format(
825
            activity = "plnt",
            mnt = month_dictionary[date_mnt_plant].strip(" ").rjust(10),
            day = date_day_plant.rjust(10),
            crp = agrl_crop_mgt.lower(),
            order = counter_mgt,
        )
        management_section_body += "{0}\n".format(management_body_line)
        counter_mgt += 1
        for agrl_crop_mgt in agrl_list:
            if plant_index == 0:
                date_day_harvest = crop_schedule_dictionary[agrl_crop_mgt].mar_harvest.
830
                date_mnt_harvest = crop_schedule_dictionary[agrl_crop_mgt].mar_harvest.
            if plant_index == 1:
                date_day_harvest = crop_schedule_dictionary[agrl_crop_mgt].aug_harvest.
                date_mnt_harvest = crop_schedule_dictionary[agrl_crop_mgt].aug_harvest.
835
            if plant_index == 2:
                date_day_harvest = crop_schedule_dictionary[agrl_crop_mgt].oct_harvest.
                date_mnt_harvest = crop_schedule_dictionary[agrl_crop_mgt].oct_harvest.
840
            split("-")[-1]
            split("-")[-1]
            if plant_index == 1:
                date_day_harvest = crop_schedule_dictionary[agrl_crop_mgt].aug_harvest.
                date_mnt_harvest = crop_schedule_dictionary[agrl_crop_mgt].aug_harvest.
845
            split("-")[-1]
            split("-")[-1]
            if plant_index == 2:
                date_day_harvest = crop_schedule_dictionary[agrl_crop_mgt].oct_harvest.
                date_mnt_harvest = crop_schedule_dictionary[agrl_crop_mgt].oct_harvest.
850
                management_body_line = ""
                {activity}{mnt}{day}      0.00000           {crp}           null      {ord
er}.00000  ".format(
855
                activity = "hvkl",
                mnt = month_dictionary[date_mnt_harvest].strip(" ").rjust(10),
                day = date_day_harvest.rjust(10),
                crp = agrl_crop_mgt.lower(),
                order = counter_mgt,

```

```

        )
    management_section_body += "{0}\n".format(management_body_line)
    counter_mgt += 1

860
    elif parts[plant_index] in crop_schedule_dictionary:
        if not parts[plant_index] == "past":

865            if plant_index == 0:
                date_day_plant = crop_schedule_dictionary[parts[plant_index]].mar_plant
            .split("-")[0]
                date_mnt_plant = crop_schedule_dictionary[parts[plant_index]].mar_plant
            .split("-")[1]
870            if plant_index == 1:
                date_day_plant = crop_schedule_dictionary[parts[plant_index]].aug_plant
            .split("-")[0]
                date_mnt_plant = crop_schedule_dictionary[parts[plant_index]].aug_plant
            .split("-")[1]
875            if plant_index == 2:
                date_day_plant = crop_schedule_dictionary[parts[plant_index]].oct_plant
            .split("-")[0]
                date_mnt_plant = crop_schedule_dictionary[parts[plant_index]].oct_plant
            .split("-")[1]
880
                management_body_line =
                    {activity}{mnt}{day}      0.00000           {crp}           null      {ord
er}.00000  ".format(
                        activity = "plnt",
885                        mnt = month_dictionary[date_mnt_plant].strip(" ").rjust(10),
                        day = date_day_plant.rjust(10),
                        crp = parts[plant_index].lower(),
                        order = counter_mgt,
                    )
                management_section_body += "{0}\n".format(management_body_line)
                counter_mgt += 1

890
                    if plant_index == 0:
                        date_day_harvest = crop_schedule_dictionary[parts[plant_index]].mar_har
895    vest.split("-")[0]
                        date_mnt_harvest = crop_schedule_dictionary[parts[plant_index]].mar_har
    vest.split("-")[1]
                        if plant_index == 1:
                            date_day_harvest = crop_schedule_dictionary[parts[plant_index]].aug_har
900    vest.split("-")[0]
                        date_mnt_harvest = crop_schedule_dictionary[parts[plant_index]].aug_har
    vest.split("-")[1]
                        if plant_index == 2:
                            date_day_harvest = crop_schedule_dictionary[parts[plant_index]].oct_har
905    vest.split("-")[0]

```

```

date_mnt_harvest = crop_schedule_dictionary[parts[plant_index]].oct_harvest.split("-")[1]

management_body_line = ""
910   {activity}{mnt}{day}      0.00000           {crp}           null      {ord
er}.00000 ".format(
    activity = "hvkl",
    mnt = month_dictionary[date_mnt_harvest].strip(" ").rjust(10),
    day = date_day_harvest.rjust(10),
    crp = parts[plant_index].lower(),
    order = counter_mgt,
)
management_section_body += "{0}\n".format(management_body_line)
counter_mgt += 1
920
if counter_mgt == 0:
    continue

management_raw += management_section_head.format(mgt_name = schedule_name, number_mana
925 l = counter_mgt, number_auto = number_of_auto_ops) + "\n" + management_section_body

# fix hrus based on dictionary

hru_data_string = """hru-data.hru: for trajectories
930 id  name          topo          hydro          soil
    lu_mgt  soil_plant_init  surf_stor  snow  field
"""
935

hru_data_hru_raw = read_from("{base}/{fn}".format(base = base_txt, fn = "hru-data.hru"))
for line in hru_data_hru_raw[2:]:
    for_part = line
    for i in range(0, 20):
        for_part = for_part.replace(" ", " ")
940    parts = for_part.split(" ")
    # print(parts[6].split("_")[0])
    hru_data_string += line.replace(parts[6], trajectories_dictionary[parts[6].split("_")[0
]].lower().replace("-", "_"))

945 write_to("{base}/{fn}".format(base = 'model_files\Scenarios\Default\TxtInOut', fn = "landus
e.lum"), landuse_lum)
write_to("{base}/{fn}".format(base = 'model_files\Scenarios\Default\TxtInOut', fn = "manage
ment.sch"), management_raw)
write_to("{base}/{fn}".format(base = 'model_files\Scenarios\Default\TxtInOut', fn = "plant.
950 ini"), plant_ini)
write_to("{base}/{fn}".format(base = 'model_files\Scenarios\Default\TxtInOut', fn = "hru-
data.hru"), hru_data_string)

```

955

960

965

Appendix B. Trajectories Description

Table 1B. Trajectories examples for each fake land-use code use for dynamic SWAT+ implementation.

Map_id	Code	Trajectory
1	TUWO	TUWO-TUWO-TUWO
2	GRAS	GRAS-GRAS-GRAS
6	BSVG	BSVG-BSVG-BSVG
11	FRST	FRST-FRST-FRST
78	BANA	BANA-BANA-BANA
110	HMEL	SHRB-SHRB-SHRB
121	INDN	CORN-BSVG-BSVG
146	LETT	CORN-BSVG-PAST
167	PAST	PAST-PAST-PAST
182	SUGC	SUGC-SUGC-SUGC
204	ASPN	FRST-BSVG-FRST
224	LIMA	CORN-PAST-PAST
225	MAPL	CORN-PAST-BSVG
243	MESQ	CORN-TOMA-PAST
248	MIGS	CORN-TOMA-BSVG
249	MINT	TOMA-TOMA-BSVG
254	MIXC	CORN-TOMA-TOMA
262	AGRR	AGRL-AGRL-AGRL

Table 2B. Dynamic agricultural land-use trajectory and their crop or vegetation cover meaning

ID	Trajectory	Crop/vegetation cover Meaning
1	CORN-PAST-PAST	rainfed maize-grass-grass

2	CORN-PAST-BSVG	rainfed maize-grass- sparse vegetation
3	CORN-TOMA-PAST	rainfed maize- tomato-grass
4	CORN-TOMA-BSVG	rainfed maize-tomato-sparse vegetation
5	AGRL-TOMA-BSVG	Beans-tomato-sparse vegetation
6	CORN-TOMA-IRR	rainfed maize-tomato-irrigated maize
7	CORN-PAST-IRR	Rainfed maize-grass-irrigated maize

970 **Table 3B. Land use classes as represented in the Static SWAT+ Model**

LANDUSE_ID	Land use Class	SWAT_CODE
1	Water	WATR
2	Grazed grassland	PAST
3	Grazed shrubland	CRGR
4	Space vegetation	BSVG
5	Rainfed Maize	CORN
6	Irrigated Sugarcane	SUGC
7	Dense forest	FRST
8	Sub_Alpine grassland	GRAS
9	Woodland	TUWO
10	Mixed Crops	AGRL
11	Irrigated Banana and Coffee	BANA
12	Wetland	WEHB
13	Urban	URMD
14	Shrubland	SHRB

975

Appendix C. Data used in this study

Table 1C. Summary of the different data used in the study with description and sources

Data Type	Description	Source/ reference
Climate	Ten station data of rainfall and four stations of maximum/minimum temperature	Tanzania Meteorological Agency (TMA) and Pangani Basin Water Office (PBWO)
Digital Elevation Model (DEM)	Elevation data from at 90m resolution	United States Geological Survey (USGS) website

Seasonal land use maps	Seasonal land use maps at 30m	(Msigwa et al., 2019)
Soil	Africa Soil Information System (AFSIS) at 250m resolution	(Hengl et al., 2015)
Remotely sensed based Actual ET	Ensemble ET from six remote sensing products	(IHE Delft, 2020)
Land management data	Planting dates, harvesting dates and irrigation application dates and frequency	Farmers interview